

# The cochlea as a smart structure

Q.1 **Stephen J Elliott<sup>1</sup> and Christopher A Shera<sup>2,3</sup>**

<sup>1</sup> Institute of Sound and Vibration Research, University of Southampton, Tizard Building, Southampton SO17 1BJ, UK

<sup>2</sup> Eaton-Peabody Laboratory of Auditory Physiology, Massachusetts Eye and Ear Infirmary, 243 Charles Street, Boston, MA 02114, USA

<sup>3</sup> Department of Otology and Laryngology, Harvard Medical School, Boston, MA 02115, USA

E-mail: [s.j.elliott@soton.ac.uk](mailto:s.j.elliott@soton.ac.uk)

Received 13 October 2011, in final form 24 January 2012

Published 9 February 2012

Online at [stacks.iop.org/SMS/21/000000](http://stacks.iop.org/SMS/21/000000)

(Ed: Lauret)

[Ascii/Word/SMS/](#)

[sms410238/SPE](#)

[Printed 9/2/2012](#)

[Spelling UK](#)

[Issue no](#)

[Total pages](#)

[First page](#)

[Last page](#)

[File name](#)

[Date req](#)

[Artnum](#)

[Cover date](#)

## Abstract

The cochlea is part of the inner ear and its mechanical response provides us with many aspects of our amazingly sensitive and selective hearing. The human cochlea is a coiled tube, with two main fluid chambers running along its length, separated by a 35 mm-long flexible partition that has its own internal dynamics. A dispersive wave can propagate along the cochlea due to the interaction between the inertia of the fluid and the dynamics of the partition. This partition includes about 12 000 outer hair cells, which have different structures, on a micrometre and a nanometre scale, and act both as motional sensors and as motional actuators. The local feedback action of all these cells amplifies the motion inside the inner ear by more than 40 dB at low sound pressure levels. The feedback loops become saturated at higher sound pressure levels, however, so that the feedback gain is reduced, leading to a compression of the dynamic range in the cochlear amplifier. This helps the sensory cells, with a dynamic range of only about 30 dB, to respond to sounds with a dynamic range of more than 120 dB. The active and nonlinear nature of the dynamics within the cochlea give rise to a number of other phenomena, such as otoacoustic emissions, which can be used as a diagnostic test for hearing problems in newborn children, for example. In this paper we view the mechanical action of the cochlea as a smart structure. In particular a simplified wave model of the cochlear dynamics is reviewed that represents its essential features. This can be used to predict the motion along the cochlea when the cochlea is passive, at high levels, and also the effect of the cochlear amplifier, at low levels.

Q.2 (Some figures may appear in colour only in the online journal)

## 1. Introduction

The ear is a remarkably sensitive and selective hearing organ. The human ear can detect sound that gives rise to internal motions of 0.3 nm, barely above Brownian motion, yet has a dynamic range of about 120 dB and a resolution of about 0.5 dB (Dallos 1996). Young people are able to hear over a frequency range of about 10 octaves, with a frequency resolution of about 0.3% of an octave. This would seem to imply an extremely resonant system, and yet we are also able to resolve timing differences, of less than 1/100 of a cycle between sounds presented to the two ears (Dallos 1996), which helps us to localize sounds. All this is achieved with a sensing cell, the inner hair cell, that in isolation has a dynamic range of only about 30 dB and an untuned frequency response.

It has been estimated that for all its impressive properties, the power consumption of the cochlea is only about 14  $\mu$ W (Sarpeshkar *et al* 1998). Although our hearing is significantly enhanced by processing of the neural signals, it is the structure of the cochlea that provides a mechanical response that is the first step towards achieving this amazing performance.

It is important to understand the mechanisms of human hearing not only because of the scientific challenges it presents, but also because such an understanding is helpful in diagnosing, and potentially treating, the multiple forms of deafness that people suffer from. Models of the cochlea assist in this understanding by allowing assumptions about how its functions should be tested; by comparing responses predicted by these models with measured data. Early measurements made of the response inside the cochlea of several species

Q.3

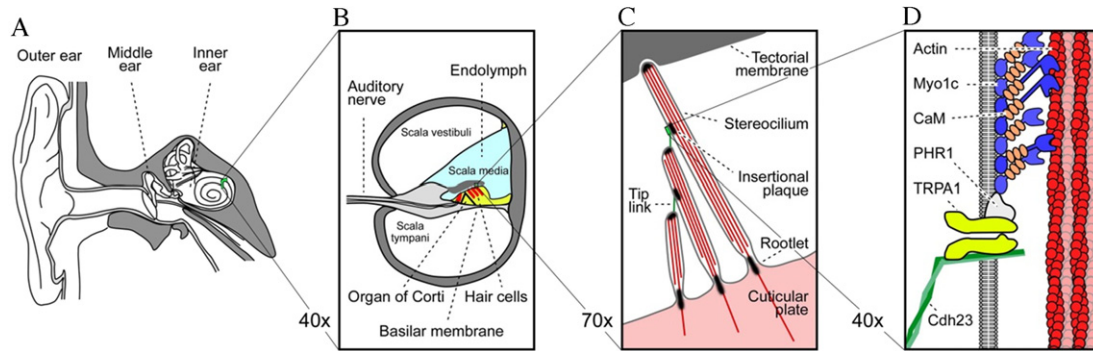


**Figure 1.** Illustrations of the structure of the inner ear at various levels of magnification. The position of the inner ear in the temporal bone is shown in (A). The cross-sectional structure within one turn of the cochlea is shown in (B), with the fluid chambers separated by the basilar membrane and the organ of Corti. The details of the bundle of stereocilia that protrude from the top of the hair cells within the organ of Corti are shown in (C). Finally (D) shows the molecular details of the myosin motors that maintain the tension in the tip links that connect the individual stereocilia within the bundle. The transduction channels (here labelled TRPA1) are now believed to reside at the bottom end of the tip link rather than the top. (Reproduced from LeMasurier and Gillespie (2005) with permission.)

were made in the pioneering work of (von Békésy 1960). Even these delicate experiments were found not to tell the whole story, however, since later measurements of the responses in living animals, as opposed to the cadaver measurements taken by von Békésy, showed sharper tuning and a significantly compressive response (Robles and Ruggero 2001). The cochlea was then recognized as having an active mechanism that amplified motion, but which only functioned at low levels and when the cochlea was physiologically intact.

Another reason to understand the cochlea is that we may want to reproduce its remarkable sensitivity and selectivity in engineering sensors. Although some authors would define a smart structure as necessarily being man-made (Spillman *et al* 1996), we take a broader definition here and consider the features of the cochlea that make what would commonly be called a smart structure (Srinivasan 1996). These features include:

- (1) an ability to sense, activate, and control motion,
- (2) an ability to adapt its responses to different conditions, and
- (3) a multi-scale structure that uses a multitude of physical processes.

The last point is illustrated in figure 1 (LeMasurier and Gillespie 2005), which shows (A) the position of the inner ear with respect to the outer and middle ear, (B) the structures of the fluid chambers and organ of Corti containing the hair cells within the inner ear, (C) the stereocilia that project from the top of the hair cells, and (D) the molecular details of the tip links that connect the stereocilia together. Different physical processes occur at each of these levels; from acoustic propagation in the ear canal, to vibration of the organ of Corti, to electrical stimulation of the hair cells by ionic flows, to molecular myosin motors that regulate the tension in the tip link. The range of these physical processes in the ear, covering the six orders of magnitude range of length-scale shown in figure 1, surely make it deserve the title of a smart structure.

The structure of the cochlea will be described in a little more detail in section 2 of this paper. A simple model of

the passive cochlea is then used in section 3 to motivate a wave description of its function, which characterizes the localization of input frequency to specific position along its length. Section 4 then discusses more detailed models of the organ of Corti that include the feedback action of the outer hair cells in the active cochlea. The use of these models in predicting otoacoustic emissions, which are important in the clinical diagnosis of deafness, is then described in section 5. The implications of this work in designing hearing prosthetics and its wider implications in designing smart sensors is then discussed.

## 2. Structure of the cochlea

The cochlea consists of a coiled labyrinth, like a snail, which is about 10 mm across and has about 2.5 turns in humans, embedded in the temporal bone of the skull. It is filled with fluid and divided into three main fluid chambers, as described, for example, by Pickles (2008), and shown in figure 1(B). The scala vestibuli is at the top, which is separated from the scala media by a thin flexible partition called Reissner's membrane, and this is itself separated from the scala tympani at the bottom by a rigid partition that includes a more flexible section, called the basilar membrane (BM).

Neither the coiling nor Reissner's membrane are believed to play a major role in the mechanics of the cochlea, however, whose dynamics can then be analysed in terms of two fluid chambers separated by the BM. The motion in the cochlea is driven by the middle ear, via a flexible window at the basal end of the upper fluid chamber, and the pressure at the basal end of the lower fluid chamber is released by another flexible window. It is thus the difference in pressure between the upper and lower fluid chambers that drives the BM into motion. The organ of Corti sits on top of the BM, and contains two types of hair cells, so-called because of the stereociliary 'hair' that projects from the top of these cells, as shown in figure 1(C). Each 10  $\mu\text{m}$ -long cross section of the organ of Corti contains a single inner hair cell (IHC), which converts the motion of the stereocilia into a chemical signal that excites adjacent

nerve fibres, generating neural impulses that then pass up the auditory pathway into the brain. There are also three rows of outer hair cells (OHC) within such a slice of the organ of Corti that play a more active role in the dynamics of the cochlea.

The individual stereocilia of a hair cell are arranged in a bundle, as shown in figure 1(C). When this bundle is deflected towards the longest unit, the fine tip links that connect the individual stereocilia are put under tension and open gating channels that let charged ions from the external fluid into the stereocilia and hence the hair cell. The current due to this ionic flow generates a voltage within the hair cell, due to its internal capacitance. In the inner hair cells, this voltage causes the cell to release a chemical neurotransmitter. When this neurotransmitter binds to receptors on nearby nerve fibres, it produces voltage changes in the fibres that, once they are above a certain threshold, trigger the nerve impulses that send signals to the brain. The effect of the corresponding motion-induced voltage in the outer hair cells is still being investigated in detail, but it is clear that it leads to expansions and contractions of the cell, which amplify the motion in the organ of Corti at low levels.

This electromotility of the outer hair cells, as it is called, is due to a unique protein on the inner surface of the cell that changes its shape when a voltage is applied, much like a piezoelectric actuator. The overall action of each outer hair cell is thus to sense motion within the organ of Corti, via its stereocilia, to control the voltage within it, via the gating channels and capacitance, and to generate a response, via electromotility. There are about 12 000 outer hair cells in the human cochlea and they each act through this mechanism as local feedback controllers of vibration. It is surprising how this large number of locally acting feedback loops can operate together to give a large and uniform amplification of the global response of the BM. It is also remarkable how quickly the outer hair cells can act, since they can respond at up to 20 kHz in humans and 200 kHz in dolphins and bats. This is much faster than muscle fibres, for example, which use a slower, climbing, mechanism to achieve contraction. Such a mechanism is still used within each stereocilium, however, to regulate the tension in the tip links and thus maintain the gating channels at the correct point in their operating curves. This is indicated in figure 1(D), in which the myosin (Myo1c) elements are shown climbing up the actin fibres to maintain tension on the gating channels (labelled TRPA1 in the figure but now no longer believed to be that protein). The molecular details of this process are still being worked out, and it is also now believed that the gating channels are on the other end of the tip links to the myosin motor (Beurg *et al* 2009). The energy for this amplification within the outer hair cells comes from the endocochlear potential, which is the 100 mV or so difference in voltage maintained between the endolymphatic fluid in the scale media and the perilymphatic fluid in the scala tympani.

### 3. Wave propagation in the passive cochlea

The frequency to place mapping that occurs within the cochlea can be described in terms of the propagation of a dispersive

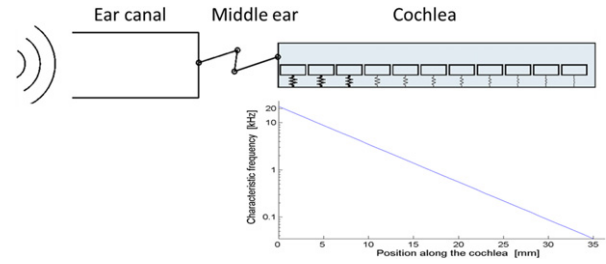


**Figure 2.** Idealized representation of the outer, middle, and inner ear, showing the BM in the inner ear as a series of mass–spring–damper systems distributed down the cochlea, together with the distribution of the natural frequencies of these single degree of freedom systems.

wave within it. This wave motion involves interaction between the inertia of the fluid chambers and the stiffness of the BM. It occurs even for excitation of the cochlea at high sound pressures, for which the active processes within the outer hair cells are saturated and do not contribute significantly to the dynamics. The fundamental wave behaviour can thus be understood in the passive cochlea, in which the feedback loops created by the outer hair cells are ignored. We begin the analysis by considering a simple ‘box model’ for the uncoiled cochlea, of length 35 mm, which has two uniform and symmetric fluid chambers and is shown in figure 2. An idealization is also shown of the ear canal, which transmits sound from the outer ear, and of the middle ear, which helps to match the mechanical impedance of waves in the air-filled ear canal and the fluid-filled inner ear. The dynamics of the BM can be approximated by a distribution of single degree of freedom, mass, spring damper, systems in this passive model. The longitudinal coupling between these elements of the BM is assumed to be weak compared with their local behaviour. The complex transverse BM velocity at a longitudinal position  $x$  and a frequency of  $\omega$ ,  $v(x, \omega)$ , then depends only on the complex pressure difference between the fluid chambers at the same position,  $p(x, \omega)$ , so that

$$v(x, \omega) = -Y_{\text{BM}}(x, \omega)p(x, \omega), \quad (1)$$

where  $Y_{\text{BM}}(x, \omega)$  is the mechanical admittance, per unit area, of the BM, and the negative sign comes from defining  $v(x, \omega)$  upwards but  $p(x, \omega)$  to be positive with a greater pressure in the upper chamber. The fluid in the cochlea is assumed to be incompressible, since the cochlear length is much smaller than the wavelength of compressional waves in the fluid, and also inviscid, since the height of the fluid chamber is much greater than the viscous boundary layer thickness, and damping is mainly introduced by the BM dynamics. The pressure is assumed to be uniform across each cross section and the conservation of fluid mass and momentum can be used to derive the governing equation for one-dimensional fluid flow in the chambers (as described, for example, by de Boer (1996)) as

$$\frac{d^2 p(x, \omega)}{dx^2} + \frac{2i\omega\rho}{h} v(x, \omega) = 0, \quad (2)$$

where  $\rho$  is the fluid density and  $h$  is the effective height of the fluid chambers, which is taken as 1 mm in the simulations

here,  $i$  is  $\sqrt{-1}$  and the complex pressure and velocity are assumed to be proportional to  $e^{i\omega t}$ . A full three-dimensional analysis of the fluid coupling which includes the finite width of the BM along the cochlea partition (Steele and Taber 1979), allows an expression for the effective height to be derived in terms of the physical dimensions of the cochlea. Such an analysis also includes a near field component of the fluid pressure, which significantly increases the apparent mass of the BM due to the entrained fluid (Neely 1985, Elliott *et al* 2011). Substituting equation (1) into (2) gives the second-order wave equation

$$\frac{d^2 p(x, \omega)}{dx^2} + k^2(x, \omega)p(x, \omega) = 0, \quad (3)$$

where the position and frequency dependent wavenumber is given by

$$k(x, \omega) = \sqrt{\frac{-2i\omega\rho}{h} Y_{BM}(x, \omega)}. \quad (4)$$

The admittance of a single degree of freedom model of the passive BM can be written as

$$Y_{BM}(x, \omega) = \frac{i\omega}{i\omega R(x) + S(x) - \omega^2 M(x)}, \quad (5)$$

where  $M(x)$ ,  $S(x)$  and  $R(x)$  are the effective mass, stiffness, and damping, per unit area, of the BM at position  $x$ . The mass per unit area is independent of the BM width, and although it does depend on the BM thickness, this only varies slowly along the length of the cochlea (Pickles 2008). This term, in any case also includes a significant component due to the entrained mass of the fluid and so it is not a bad approximation to assume that the BM mass is constant along its length, which is here denoted  $M_0$ , and is taken to be have a value of  $0.3 \text{ kg m}^{-2}$ . The distribution of natural frequencies along the cochlea is approximately exponential, so we assume that

$$\omega_n(x) = \omega_0 e^{-x/l}, \quad (6)$$

where  $l$  is a characteristic length, taken here to be 7 mm and  $\omega_0$  the natural frequency at the base of the cochlea, taken here to be  $2\pi$  times 20 kHz. The distribution of natural frequencies,  $\omega_n(x)$ , illustrated in figure 2 is assumed to be entirely due to the longitudinal variation of the BM stiffness, so that the distribution of BM stiffness is then given by

$$S(x) = \omega_0^2 M_0 e^{-\frac{2x}{l}}. \quad (7)$$

We also assume that the damping ratio of the BM is constant along its length, which is generally characterized in the cochlea community by its  $Q$  factor, which is assumed to be constant along the cochlear length and to have a value,  $Q_0$ , of 2.5 here. The distribution of the mechanical damping is then

$$R(x) = \frac{\omega_0 M_0}{Q_0} e^{-\frac{x}{l}}. \quad (8)$$

Since the wavenumber varies with position and frequency, conventional solutions to the wave equation, for homogeneous systems, cannot be used. Provided the wavenumber does not change too rapidly compared with the wavelength, however,

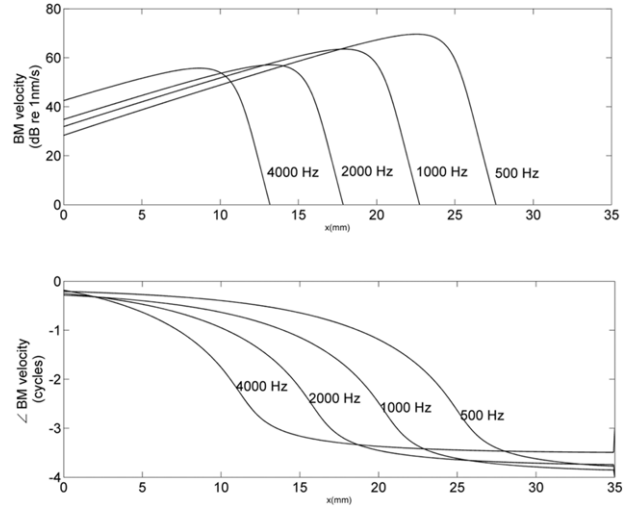


**Figure 3.** Simulations of the distribution along the length of the passive cochlea of the magnitude and phase of the complex BM velocity, when excited at the stapes by pure tones of different frequencies.

an approximate global solution for  $v(x, \omega)$  can still be obtained using the WKB method (Zweigt *et al* 1976) as

$$v(x, \omega) \approx A k^{\frac{3}{2}}(x, \omega) e^{-i \int_0^x k(x', \omega) dx'}, \quad (9)$$

where  $A$  is the amplitude, due to the driving velocity from the middle ear. It is found that, to a very good approximation, only a forward-travelling wave exists if the cochlea has smoothly varying parameters (De Boer and MacKay 1980), since this is almost perfectly absorbed as it travels along the cochlea, thus ensuring an optimum transfer of power from the middle ear. Figure 3 shows the modulus and phase of the BM velocity, as a function of position along the cochlea, for four different driving frequencies, calculated using a finite difference approximation to equation (3) for the passive BM (Neely and Kim 1986, Young 2011). The phase is plotted in cycles, as is customary in the hearing literature, which, perhaps, should be adapted more widely since it has more immediate physical significance than either radians or degrees. One of the main features of the BM velocity distributions in figure 3 is that they peak at different places for different excitation frequencies, providing a ‘tonotopic’ distribution of frequency.

The position of the peak at each frequency can be understood by considering the form of the local wavenumber in equation (4) at different positions, for a given excitation frequency. We first define the place along the cochlea where the BM natural frequency is equal to the excitation frequency as  $x_n$ . If  $x$  is significantly less than  $x_n$ , the BM will be stiffness controlled, so that  $Y_{BM}(x, \omega)$  is approximately equal to  $i\omega/S(x)$  and the wavenumber in equation (4) is entirely real and equal to  $\omega/c(x)$  where  $c(x)$  is the local wave speed given by

$$c(x) = \sqrt{\frac{h S(x)}{2\rho}}. \quad (10)$$

The wave speed thus drops off as the wave propagates along the cochlea, since  $S(x)$  falls with increasing  $x$ , as in equation (7). The wave amplitude then builds up as it travels towards  $x_n$ , just as the amplitude of a water wave does at it approaches a beach, so that its energy is conserved. For positions well beyond  $x_n$ , however, the response of the BM will be mass controlled, so that  $Y_{BM}(x, \omega)$  is approximately equal to  $1/i\omega M_0$  and the wavenumber is entirely imaginary, and corresponds to an evanescent decay with a characteristic length of

$$d = \sqrt{\frac{hM_0}{2\rho}}, \quad (11)$$

which is about 1 mm for the parameters assumed here. If  $x$  is equal to  $x_n$ ,  $Y_{BM}(x, \omega)$  is dominated by the damping, and the wavenumber has equal real and imaginary parts, which represents the transition between the propagating wave, when  $x$  is less than  $x_n$ , and the evanescent wave, when  $x$  is greater than  $x_n$ . Since the natural frequency of the BM varies exponentially along the length of the cochlea, as shown in figure 2, the position of the peak BM response is thus inversely proportional to the log of the frequency.

At a given frequency, the real part of the wavenumber in the passive cochlea thus starts out with a small value near the base, increases along the cochlea to a peak at about  $x_n$  and then decays to zero. The magnitude of the imaginary part of the wavenumber is very small near the base and abruptly increases in magnitude near  $x_n$ , before falling to a constant value. The imaginary part of the wavenumber is always negative in the passive cochlea, since power can only be dissipated as it travels along. If the natural frequencies are spread out exponentially, as in equation (6), then the spatial distribution of this wavenumber, at a constant frequency, has exactly the same form as the distribution of the wavenumber with log frequency, at a given position; a feature which is known as scaling symmetry.

The distribution of wavenumbers can be directly inferred from the measured frequency response of the BM velocity at a given location using an inversion procedure described by Shera (2007). Figure 4 shows the distribution of the real and imaginary parts of the wavenumber calculated using such a procedure, based on the BM velocity measured for low excitation levels at seven different locations in the cochlea of a chinchilla (Shera 2007). The real parts of the wavenumber, given by the black lines in figure 4, show the trend expected from the analysis of the passive cochlea; gradually increasing and then falling off. The peak value can be used to calculate the minimum wavelength, which falls from about 1 mm near the base to 3 mm further along. The important difference between the measured results and those predicted from the passive theory, however, is in the distribution of the imaginary part of the wavenumber, shown by the grey lines. This is predicted always to be negative in the passive cochlea, but is clearly positive just before the peak position in the data inferred from the measurements. This indicates that power is being supplied to the wave at these positions, which amplifies the wave just before its peak, and is clear evidence for an active mechanism within the cochlea.

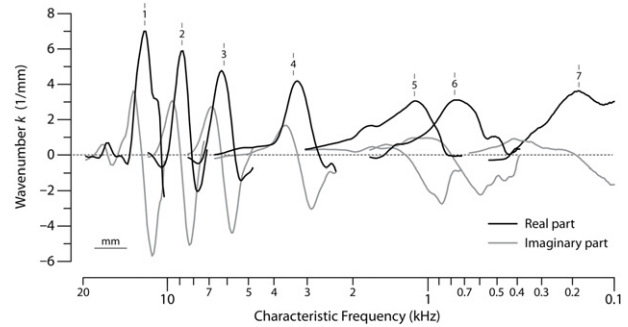


**Figure 4.** The distribution of the real, black, and imaginary, grey, parts of the wavenumber inferred from measurements of the BM frequency response at seven positions along the length of the cochlea using an inversion procedure (after Shera 2007).

#### 4. The active cochlea

The motion of the BM is enhanced by the feedback action of the outer hair cells at low sound pressure levels. The detailed process by which this occurs is not completely understood, but the basic mechanism can be explained with reference to the structure of the organ of Corti shown on the left-hand side of figure 5. As the BM moves upwards, the stereocilia of the outer hair cells, OHC, are deflected by the shearing motion between the reticular lamina, RL, and the tectorial membrane, TM. This modulates the ionic flow through the gating channels associated with the tip links, altering the voltage inside the electromotile outer hair cells and thus causing them to change their length. This length change will itself generate a deflection of the stereocilia, and so the micromechanics of the organ of Corti have to be considered as a closed-loop feedback system.

A number of lumped parameter models have been put forward to describe the mechanics of this micromechanical system, with various numbers of degrees of freedom used to approximate the continuous physical system. Figure 5 also shows one such model (Geisler and Sang 1995, Ramamoorthy *et al* 2007, Elliott 2009), in which the outer hair cells react between the lumped BM and RL, forcing the TM upwards and generating a shearing action on the OHC stereocilia. The radial motion of the TM can be transformed into an equivalent vertical degree of freedom using the geometry of such a model (Allen 1980), to give the lumped parameter model on the right in figure 5. This active micromechanical model only changes the form of the BM admittance in the equation for the wavenumber, (4), since the fluid coupling in the box model remains the same, and so the WKB expression in equation (9) for the overall BM velocity remains the same, but with a modified distribution of  $k(x)$ .

By assuming that the RL mass is significantly less than that of the BM or TM, the order of this model can be reduced so that it has only two degrees of freedom. The action of the outer hair cells can also be incorporated by assuming that the force they generate between the BM and RL is proportional to the resolved shearing motion between the RL and TM. The feedback loop generated by the outer hair cells, from displacement to force, provides an active input but

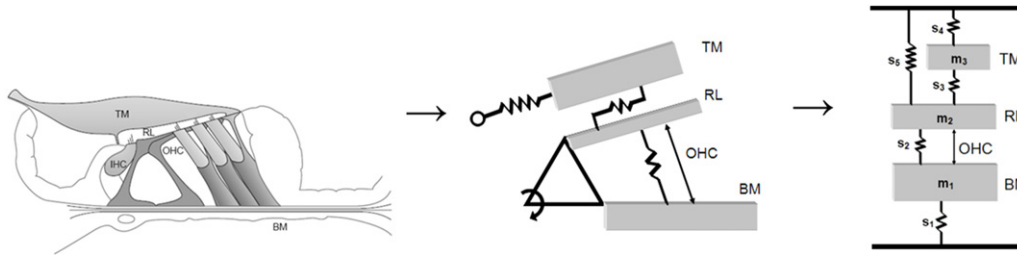


**Figure 5.** The three stages of development of the lumped parameter micromechanical model. A cross section of the physical arrangement of the cochlear partition is shown on the left, including the basilar membrane (BM), outer hair cells (OHC), reticular lamina (RL) and tectorial membrane (TM). The middle figure illustrates how these components are assumed to move relative to each other in a lumped parameter model, in which the old-style resistance symbols denote lossy springs. The transverse BM motion is driven both by the pressure difference in the fluid chambers and the force due to the OHC, and the TM moves transversely and radially, driven by the OHC via the RL. The forces due to this radial motion can be resolved into equivalent transverse forces and the radial TM degree of freedom can be represented as an equivalent transverse degree of freedom, as shown in the final lumped parameter model shown in the right-hand figure.

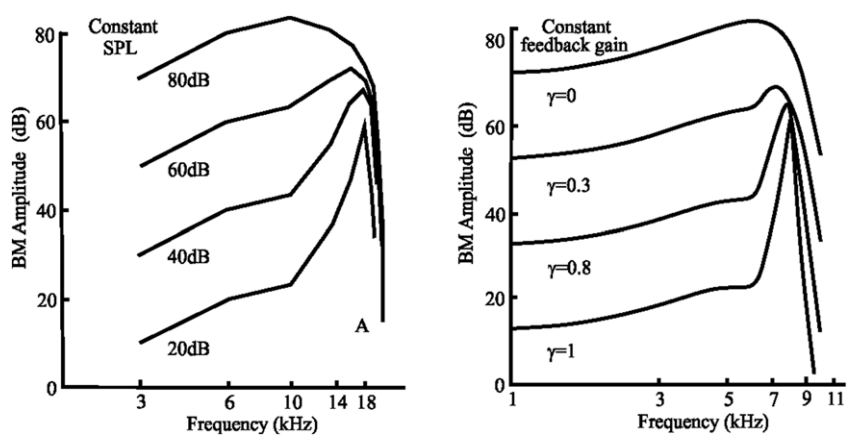


**Figure 6.** The measured frequency response of the BM displacement, left, for various levels of acoustic excitation at one point on the BM (reproduced from Johnstone *et al* (1986) with permission). The simulated frequency responses for various values of the feedback gain in a model of the active cochlea are shown on the right, each offset by 20 dB for comparison with the measurements.

does not add any inertial element to the lumped parameter model, which then still has only two degrees of freedom. A passive two degree of freedom system has one complex conjugate pair of zeros positioned between the two complex conjugate pairs of poles that define the response of its two modes. This alternating pole-zero structure ensures that the real part of the input admittance is always positive (Preumont 2011). The action of the outer hair cells breaks this passive constraint, however, allowing the real part of the admittance to be negative at frequencies just below the main resonance frequency. This provides a mechanism for supplying power to the cochlea travelling wave just before it reaches its peak value and thus significantly increasing its amplitude.

The left-hand side of figure 6 shows the values of the BM displacement, measured at a single place on the BM at different frequencies and for various levels of exciting sound (Johnstone *et al* 1986). These very delicate measurements can only be made in the physiologically intact cochleae of experimental animals. The results shown in figure 6 were made in a guinea pig, at a place where the frequency of peak response was about 18 kHz. These measurements have a very similar shape at similar positions in a number of different laboratory animals (Robles and Ruggero 2001).

Q.4

The right-hand side of figure 6 shows the results of a simulation of such an active cochlear model (Young 2011) with four values of the normalized feedback gain,  $\gamma$ , in the feedback loop provided by the outer hair cells. The frequency of peak response here is about 8 kHz, since it is a human cochlea that is being simulated. For  $\gamma$  equal to zero the cochlea is passive and the log frequency response shown in figure 6 is equivalent to the spatial distribution at a single frequency shown in figure 3, because the log frequency scales exactly with position in this model. As  $\gamma$  is increased, the outer hair cells provide an increasing amplification of the response at frequencies slightly higher than the peak in the passive response, which rises to about 40 dB with the normalized gain,  $\gamma$ , equal to 1. The responses for each value of  $\gamma$  are offset by 20 dB to allow comparison with the measured results. The general form of the measured results is reproduced reasonably well in these simulations of the active cochlea, although some of the details, particularly the change with level above the active peak, are not. Enhancement of the response is due to positive feedback, and so there must be a concern for the stability of such a system. By casting the dynamics in state space form, the position of the poles for the coupled system can be determined (Elliott *et al* 2007) and hence the maximum stable feedback gain calculated. For the

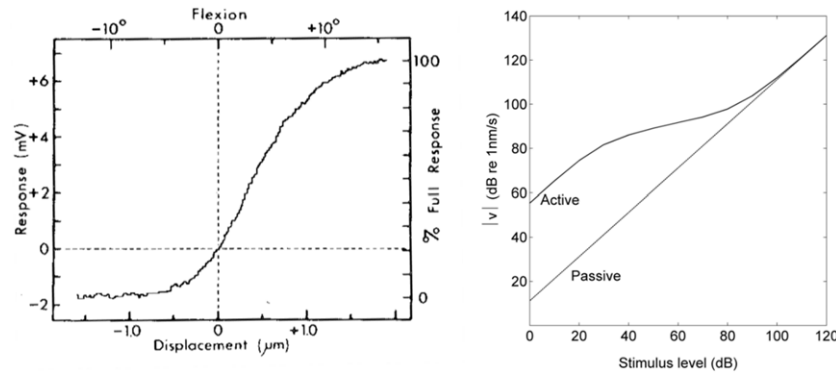


**Figure 7.** The nonlinear response, left, from stereocilia deflection to electrical response, of the mechanoelectric transduction within a hair cell (reproduced from Hudspeth and Corey (1977) with permission). The right-hand graph shows the level of the BM velocity plotted against the level of the acoustic excitation, from a simulation of the active nonlinear cochlea that incorporates a similar nonlinearity within the feedback control loops (Young 2011). The feedback control loops amplify the velocity response by about 40 dB at low excitation levels, but by a decreasing amount as the level is increased, as a result of saturation, producing a significant compression of the dynamic range.

model considered here, this maximum stable feedback gain corresponds to a normalized gain of about 1.007. This model of the coupled system thus has a gain margin of only about 0.06 dB when it is acting to amplify the BM motion by 40 dB, which is very small when one considers the normal variability of biological systems. It is probably one of the functions of the stereocilia tip links to regulate the operating point of the outer hair cells in order to maintain this degree of amplification without catastrophic instability, but the mechanism by which this occurs is unclear.

The outer hair cells only provide full amplification at low sound pressure levels. As the sound pressure levels increase, the Boltzmann-like nonlinearity of the gating channels in the hair cells, illustrated on the left-hand side of figure 7, reduces the effective gain of the feedback loops, so that at very high sound pressure levels the gain tends to zero and the cochlea becomes entirely passive. The reduction in feedback gain with increasing level can be analysed at a single frequency using a describing function analysis of the nonlinearity, for example. This was used to adjust the feedback gains used in figure 6, for the various sound pressure levels used in the experimental measurements of BM velocity frequency response at different levels. The saturating nonlinearity of the cochlea amplifier thus reduces the positive feedback gain with level (Yates 1990, Cooper 2004). The right-hand side of figure 7 shows the calculated level of the peak BM velocity as a function of the sound pressure level used to excite a model that incorporates such a nonlinearity. This level curve shows similar characteristics to those taken from direct measurements on the BM (Robles and Ruggiero 2001). The dashed line shows the level curve for a linear passive cochlea, with a constant slope of 1 dB/dB. The active response tends towards this passive curve for sound pressure levels above about 90 dB, when the nonlinearity is completely saturated. At low levels, the BM velocity is amplified by about 40 dB in this case, due to the positive feedback from the outer hair cells. This amplification begins to reduce as the sound pressure level increases beyond about 30 dB, due to saturation of the outer hair cell nonlinearity. A 60 dB increase in sound pressure level thus produces only about a 20 dB increase in

the level of BM velocity. There are a number of mechanisms for the compression of dynamic range within the cochlea, but the nonlinearity of the outer hair cells is a particularly important one, since it operates over the range of levels of most natural sounds. All of these forms of compression are important, however, since together they reduce the 120 dB or so dynamic range of sound pressure level over which we can hear at mid-frequencies, from the threshold of hearing to the threshold of pain, to the 30 dB or so dynamic range over which the inner hair cells can efficiently transform motion into neural signals (Dallos 1996).

The nonlinearity of the transducer channels in the outer hair cells provides one mechanism by which the cochlea can adapt its response to different conditions, principally the sound pressure level in this case. Another potential mechanism for adaptation is via the ‘efferent’ nerves that carry signals back down from the central nervous system into the cochlea, and, particularly, into the outer hair cells. The functional role of these pathways is not understood, but it is believed that they may protect the cochlea from acoustic trauma, assist in the discrimination of different sounds, especially in background noise, and that they have a role in modifying the response of the cochlea in response to the attention paid to particular sounds (Guinan 1996, Pickles 2008).

## 5. Otoacoustic emissions

A fascinating—and, as it turns out, extremely useful—by-product of active wave amplification in the cochlea is that the ear makes sound while listening to sound. Sounds evoked from the ear, known as ‘otoacoustic emissions’ (OAEs), can be recorded in the ear canals of most normal hearing listeners using sensitive, low-noise microphones. These sounds are believed to result from the generation of backward-travelling waves within the cochlea, which are then transmitted in the reverse direction through the middle ear to the ear canal. Although forward-travelling waves dominate the cochlear response, mechanical irregularities or impedance variations

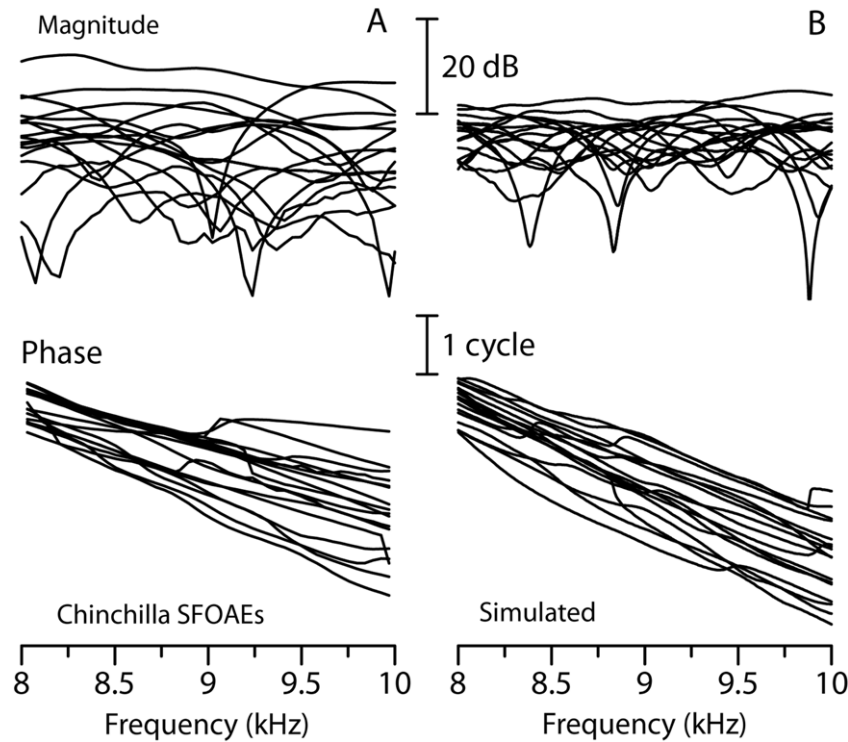


**Figure 8.** Measured and simulated single frequency otoacoustic emission (SFOAE) spectra. Panel (A) shows measured magnitudes and phases of the emissions evoked by a low level pure tone in 17 chinchillas reported by Siegel *et al* (2005). Panel (B) shows the emissions computed using a model with parameter values chosen to match chinchilla wavenumbers (see figure 4). Emissions in 17 different ‘subjects’ were simulated by using different random patterns of mechanical irregularities. (Reproduced with permission from Shera *et al* (2008).)

due to the nonlinear dynamics can ‘scatter’ the forward wave, producing micro-reflections. In the active system, these reflected wavelets can themselves be amplified, just like the main forward-travelling wave. When the wavelets scattered from different places combine coherently, they can yield a significant net backward-travelling wave and produce measurable emissions (e.g. Zweig and Shera 1995). Figure 8 shows that models incorporating these ideas are able to reproduce measured emission spectra. The figure compares measured and model simulations of the emissions evoked by a low level pure tone. The wavenumbers in the model were chosen to match those derived from chinchilla data (see figure 4), and the mechanical irregularities that scatter the waves were assumed to vary randomly with position. Overall, there is excellent agreement between the model and the measurements. Note that the emission phase falls through multiple cycles, a result of delays arising from frequency tuning and round-trip wave propagation in the cochlea.

Sometimes the wave scattering can run away with itself through a process of multiple internal reflection. At the basal end of the cochlea, where the cochlea and the middle ear join up, there is an impedance mismatch that can reflect travelling waves. Thus, when backward-travelling waves created by scattering reach the middle ear, they are partially reflected back into the cochlea, generating a new forward-travelling wave. This new wave will in turn be amplified and then scattered by mechanical irregularities along its path, generating another backward-travelling wave, and so on. When the gain provided by the cochlear amplifier

is sufficiently high, and when the round-trip phase shift due to wave travel is an integral number of cycles, the multiple internal reflections can reinforce one another and create self-sustaining standing waves inside the cochlea whose amplitude is limited by the saturation of the outer hair cell forces. In the ear canal, these standing waves can be heard as a series of narrow-band pure tones emitted from the ear at levels close to the threshold of hearing (see figure 9). The reflection and amplification processes responsible for the generation of these so-called spontaneous otoacoustic emissions represent an acoustic and biological analogue of the generation of light by an optical laser (Shera *et al* 2003).

Otoacoustic emissions are not just an academic curiosity; they provide a noninvasive window on the mechanics of the cochlea. OAEs are already routinely used in the clinical screening of infants for hearing problems. They also serve a valuable role in testing cochlear models (e.g. figure 8). Although comparison with direct measurements of BM velocity response in laboratory animals provides the most obvious way of validating a model’s response, the use of invasive measurements is problematic for models of the human ear, both because the measurements are always performed on laboratory animals (i.e. on some other species whose cochlea may be different) and because there are invariably concerns about the physiological state of the cochlea in such experiments. Otoacoustic emissions can be useful here. Because their measurement is noninvasive and can be performed without physiological intrusion they provide an attractive way of performing ‘non-destructive testing’ on

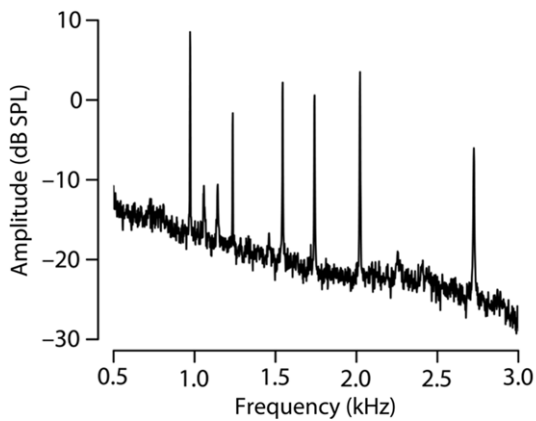


**Figure 9.** Whistling while it works: a power spectrum showing spontaneous otoacoustic emissions from the cochlea recorded in the external ear canal. The spectral peaks indicate the presence of narrow-band acoustic signals close to the threshold of hearing, which are thought to arise via active, standing-wave resonances within the inner ear.

the human cochlea in the hope of measuring its fundamental properties.

The use of otoacoustic emissions to provide noninvasive estimates of the sharpness (or  $Q$  factors) of cochlear tuning provides an example of the scientific utility of OAEs. Cochlear models of the type discussed above predict that OAE delays are determined largely by the bandwidth of the mechanical frequency response of the BM—the narrower the relative tuning bandwidths, the longer the response build-up and decay times, and thus the longer the otoacoustic group delays. The predicted correlations between tuning and OAE delay have been validated in animal models where both types of data can be measured. Since human OAE delays are exceptionally long (e.g. a factor of 2 or 3 longer than in guinea pigs or chinchillas), the same reasoning implies that human cochlear tuning is sharper than in common laboratory animals (Shera *et al* 2002, 2010). Although behavioural measurements can be significantly affected by neural processing in the brain, and generally involve a great deal more than just peripheral mechanics, similar conclusions about human cochlear tuning were subsequently obtained using psychoacoustic procedures designed to mimic the measurement of neural tuning curves (Oxenham and Shera 2003).

## 6. Discussion and conclusions

Dispersive wave motion in the inner ear generates a tonotopic mapping of frequency onto position along the cochlea. The signals at these positions are then coded by the inner hair cells for neural processing along the auditory pathway into the brain. The cochlea has nonlinear active processes that amplify the response to low sound levels, giving extreme sensitivity, but which also saturate at higher sound levels, to provide a wide dynamic range. The structure and activity of the inner ear thus significantly enhances the sensory capabilities of the 3000 or so inner hair cells. The outer hair cells sense, actuate, and control motion within the inner ear. Their nonlinearity

also allows the ear to adapt its response to different conditions, particularly changes in level, and this is achieved with a multi-scale structure using a variety of physical processes. The ear clearly satisfies the criterion for a smart structure.

Although an understanding of normal cochlear mechanics is of fundamental scientific interest, it can also be used to help understand the effects of different forms of hearing impairment and perhaps even inspire devices to help overcome these impairments. Modern hearing aids and cochlear implants generally work by dividing the sound signal into frequency bands and applying some nonlinear compression of the dynamic range within each band (Moore 2003). Although this mimics part of the action of the healthy cochlea (the dynamic range compression), it does not restore the sharp frequency resolution produced by the active mechanics. Since active filtering appears crucial for discriminating sounds in background noise, current technologies for aiding the impaired ear can return sounds to audibility but cannot yet restore normal hearing.

Physical models of cochlear mechanics were originally built to help understand the mechanism of cochlear action, and were either mechanical (von Békésy 1960) or electrical (Zwicker 1986). Interest then developed in miniaturized devices that mimicked cochlear action (e.g. Lyon and Mead 1988), which could potentially be used as signal processing devices for hearing aids and cochlear implants (e.g. White and Grosh (2005) who used a MEMS device). More generally, the wave nature of frequency discrimination in the cochlea has been suggested as an efficient form of spectrum analysis (Mandal *et al* 2009). These authors have presented a particularly interesting discussion of the efficiency of the travelling wave method of frequency analysis, as used in the cochlea, compared with filter banks and the FFT algorithm. Figure 10 illustrates how, in order to resolve  $N$  different frequencies, a filter bank requires  $N$  filters each of order about  $N$ , requiring a processing power of order  $N^2$ . The FFT algorithm can compute  $N$  frequency bands with a processing power of order  $N \log N$ . The travelling wave approach, however, can use the same set of  $N$  elements to analyse each of  $N$  frequency bands, and so only requires a processing power of order  $N$ . Mandal *et al* (2009) use a CMOS implementation of a circuit model of wave propagation, with linear active circuits having two degrees of freedom for amplification. Instead of designing their circuit to work in the audio range, however, these authors have implemented a radio frequency device, working up to 8 GHz, to illustrate the efficiency of this wave approach. This paper gives one of the clearest indications that the wave nature of frequency discrimination on the cochlea may have more general engineering application in spectral analysis.

Although these mechanical and electrical models can reproduce the linear response of the cochlea reasonably well, and Mandal *et al* (2009) implementation also reproduces the active response, the full nonlinearity of the cochlear response is not yet well modelled. It is clear from figure 6 that the sharpness of the real cochlear response increases at lower excitation levels, and this happens fairly independently at each place along the cochlea, giving rise to a dynamically changing

Q.5

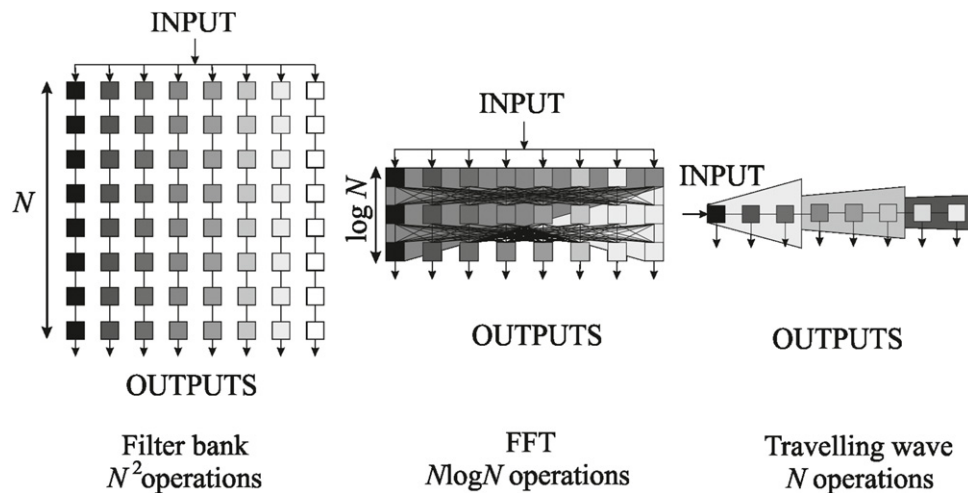


**Figure 10.** Three methods of analysis of a signal into  $N$  spectral components, with low frequencies being denoted by darker squares and high frequencies by lighter squares, and the order of magnitude of the processing power this requires; by using a filter bank (left), by using an FFT algorithm (centre), and using a travelling wave approach (right) (after Mandal *et al* 2009).

filter bank that is particularly well suited to detecting low level speech cues in high levels of background noise (Allen *et al* 2008). In fact the response of the cochlea is even more elegant than this, since, in contrast to its amplitude response, its measured phase response is almost independent of excitation level (Robles and Ruggero 2001), so that the zero crossings of the cochlea's impulse response are also independent of level (Shera 2001). Thus, although the compressive nonlinearity generated by the saturation of the outer hair cells will boost the low level frequency components of the signal, the relative timing information between the ears, required for accurate sound localization, is preserved. A great deal of sophisticated signal processing is thus performed by the action of the cochlea as a smart structure, even before the signals are neurally encoded and passed up the auditory pathway. Further study of the detailed behaviour of the cochlea's nonlinear dynamics could usefully inform algorithms for speech detection and recognition. It is the distributed nature of both the frequency selectivity and the nonlinearity within the cochlea that helps provide such a remarkable front end to our sense of hearing.

The study of the inner ear thus not only provides a sobering example of the complexity of a biologically smart structure, but can also be used to inspire engineered sensors, prostheses, and signal processors with novel capabilities.

## Acknowledgments

The simulation results in figures 3, 6, and 7 were kindly provided by J Young, based on the model in her PhD thesis (Young 2011). Thanks are also given to Ni Guangjian for assistance with the figures.

## References

- Allen J B 1980 Cochlear micromechanics—a physical model of transduction *J. Acoust. Soc. Am.* **68** 1660–70
- Allen J B, Regnier M and Li F 2008 Nonlinear cochlear signal processing and phoneme perception *Concepts and Challenges in the Biophysics of Hearing* ed N P Cooper and D T Kemp, pp 93–105
- Beurg M, Fettiplace R, Nam J H and Ricci A J 2009 Localization of inner hair cell mechanotransducer channels using high-speed calcium imaging *Nature Neurosci.* **12** 553–8
- Cooper N P 2004 Compression in the peripheral auditory system *Compression: From Cochlea to Cochlea Implants* ed R D Bacon, R F Fay and A M Popper (Berlin: Springer) pp 18–61
- Dallos P 1996 *The Cochlea* ed P Dallos, A N Popper and R R Fay (Berlin: Springer) Chapter 1 (Overview: Cochlear Neurobiology) pp 1–43
- de Boer E 1996 *The Cochlea* ed P Dallos, A N Popper and R R Fay (New York: Springer) Chapter (Mechanics of the Cochlea: Modelling Efforts) pp 258–317
- De Boer E and MacKay R 1980 Reflections on reflections *J. Acoust. Soc. Am.* **67** 882–90
- Elliott S J 2009 Active control of vibration in aircraft and inside the ear *Active 2009 Conference (Ontario)*
- Elliott S J, Ku E M and Lineton B 2007 A state space model for cochlear mechanics *J. Acoust. Soc. Am.* **122** 2759–71
- Elliott S J, Lineton B and Ni G 2011 Fluid coupling in a discrete model of cochlear mechanics *J. Acoust. Soc. Am.* **130** 1441–51
- Geisler C D and Sang C 1995 A cochlear model using feed-forward outer-hair-cell forces *Hear. Res.* **86** 132–46
- Guinan J J Jr 1996 *The Cochlea* ed P Dallos, A N Popper and R R Fay (Berlin: Springer) Chapter 8 (Physiology of Olivocochlear Efferents) pp 435–502
- Hudspeth A J and Corey D P 1977 Sensitivity, polarity, and conductance change in the response of vertebrate hair cells to controlled mechanical stimuli *Proc. Natl Acad. Sci.* **74** 2407–11
- Johnstone B M, Patuzzi R and Yates G K 1986 Basilar membrane measurements and the travelling wave *Hear. Res.* **22** 147–53
- LeMasurier M and Gillespie P G 2005 Hair cell mechanotransduction and cochlear amplification *Neuron* **48** 403–15
- Lyon R F and Mead C 1988 An analog electronic cochlea *IEEE Trans. Acoust. Speech Signal Process.* **36** 1119–34
- Mandal S, Zhak S M and Sarpeshkar R 2009 A bio-inspired active radio-frequency silicon cochlea *IEEE J. Solid State Circuits* **44** 1814–28

Q.7

Q.8

- Moore B C J 2003 *Cochlear Hearing Loss* (London: Whurr Publishers)
- Neely S T 1985 Mathematical modelling of cochlear mechanics *J. Acoust. Soc. Am.* **78** 345–52
- Neely S T and Kim D O 1986 A model for active elements in cochlear biomechanics *J. Acoust. Soc. Am.* **79** 1472–80
- Oxenham A J and Shera C A 2003 Estimates of human cochlear tuning at low levels using forward and simultaneous masking *JARO* **4** 541–54
- Pickles J O 2008 *An Introduction to the Physiology of Hearing* 3rd edn (Bingley: Emerald)
- Preumont A 2011 *Vibration Control of Active Substances: An Introduction* 3rd edn (Berlin: Springer)
- Ramamoorthy S, Deo N V and Grosh K 2007 A mechano-electro-acoustical model for the cochlea: response to acoustic stimuli *J. Acoust. Soc. Am.* **121** 2758
- Robles L and Ruggero M A 2001 Mechanics of the mammalian cochlea *Physiol. Rev.* **81** 1305–52
- Sarpeshkar R, Lyon R F and Mead C 1998 A low-power wide-dynamic-range analog VLSI cochlea *Analog Integr. Circuits Signal Process.* **16** 245–74
- Shera C A 2001 Intensity-invariance of fine time structure in basilar-membrane click responses: implications for cochlear mechanics *J. Acoust. Soc. Am.* **110** 332–48
- Shera C A 2003 Mammalian spontaneous otoacoustic emissions are amplitude-stabilized cochlear standing waves *J. Acoust. Soc. Am.* **114** 244–62
- Shera C A 2007 Laser amplification with a twist: traveling-wave propagation and gain functions from throughout the cochlea *J. Acoust. Soc. Am.* **122** 2738–58
- Shera C A, Guinan J J Jr and Oxenham A J 2002 Revised estimates of human cochlear tuning from otoacoustic and behavioural measurements *Proc. Natl Acad. Sci.* **99** 3318–23
- Shera C A, Guinan J J Jr and Oxenham A J 2010 Otoacoustic estimation of cochlear tuning: validation in the Chinchilla *JARO* **11** 343–65
- Shera C A, Tubis A and Talmadge C L 2008 Testing coherent reflection in chinchilla: auditory-nerve responses predict stimulus-frequency emissions *J. Acoust. Soc. Am.* **124** 381–95
- Siegel J H, Cerka A J, Recio-Spinoso A, Temchin A N, van Dijk P and Ruggero M A 2005 Delays of stimulus-frequency otoacoustic emissions and cochlear vibrations contradict the theory of coherent reflection filtering *J. Acoust. Soc. Am.* **118** 2434–43
- Spillman W B Jr, Sirkis J S and Gardiner P T 1996 Smart materials and structures: what are they? *Smart Mater. Struct.* **5** 247–54
- Srinivasan A V 1996 Smart biological systems as models for engineered structures *Mater. Sci. Eng. C* **4** 19–26
- Steele C R and Taber L A 1979 Comparison of WKB calculations and experimental results for three-dimensional cochlear models *J. Acoust. Soc. Am.* **65** 1007–18
- von Bekesy G 1960 *Experiments in Hearing* (New York: McGraw Hill) (Reissue Bekesy von G 1989 Acoust. Soc. Am.)
- White R D and Grosh K 2005 Microengineered hydromechanical cochlear model *Proc. Natl Acad. Sci.* **102** 1296–301
- Yates G K 1990 Basilar membrane nonlinearity and its influence on auditory nerve rate-intensity functions *Hear. Res.* **50** 145–62
- Young J A 2011 Modelling the cochlear origins of distortion product otoacoustic emissions *PhD Thesis* University of Southampton
- Zweig G, Lipes R and Pierce J R 1976 The cochlear compromise *J. Acoust. Soc. Am.* **59** 975–82
- Zweig G and Shera C A 1995 The origin of periodicity in the spectrum of evoked otoacoustic emissions *J. Acoust. Soc. Am.* **98** 2018
- Zwicker E 1986 A hardware cochlear nonlinear preprocessing model with active feedback *J. Acoust. Soc. Am.* **80** 146–53

## Queries for IOP paper 410238

Journal: SMS  
Author: S J Elliott and C A Shera  
Short title: The cochlea as a smart structure

### Page 1

---

#### Query 1:

Author: Please check the author names and affiliations carefully.

### Page 1

---

#### Query 2:

Author: Please be aware that the colour figures in this proof will normally only appear in colour in the online Web version. If you require colour in the printed journal and have not previously arranged it, please contact the Publishing Administrator now.

### Page 1

---

#### Query 3:

Author: 'Sarpeskar *et al* 1998' changed to 'Sarpeshkar *et al* 1998' as per reference list. Please check.

### Page 6

---

#### Query 4:

Author: 'Johnson *et al* 1986' changed to 'Johnstone *et al* 1986' here and in similar cases as per reference list. Please check.

### Page 9

---

#### Query 5:

Author: 'Moore 1998' changed to 'Moore 2003' as per reference list. Please check.

### Page 10

---

#### Query 6:

Author: Please check the details for any journal references that do not have a blue link as they may contain some incorrect information. Pale purple links are used for references to arXiv e-prints.

### Page 10

---

#### Query 7:

Author: Allen *et al* (2008): Please provide place and publisher.

### Page 11

---

#### Query 8:

Author: Oxenham and Shera (2003), Shera (2010): Please check the journal title given here.